Communication

The Relationship Between Microstructural Evolution and Mechanical Properties of Heavy Plate of Low-Mn Steel During Ultra Fast Cooling

BIN WANG, ZHAO-DONG WANG, BING-XING WANG, GUO-DONG WANG, and R. D. K. MISRA

We describe here the electron microscopy and mechanical property studies that were conducted in an industrially processed 20- and 40-mm C-Mn thick plates that involved a new approach of ultrafast cooling (UFC) together with significant reduction in Mn-content of the steel by ~0.3 to 0.5 pct, in relation to the conventional C-Mn steels, with the aim of cost-effectiveness. The study demonstrated that nanoscale cementite precipitation occurred during austenite transformation in the matrix of heavy plate during UFC, providing significant precipitation strengthening. With decrease in UFC stop temperature and consequent increase in the degree of undercooling, there was a transition in the morphology of cementite from lamellar to irregular-shaped nanoscale particles in the 20 mm heavy plate. With the increase in plate thickness, nanoscale cementite precipitated in bainitic lath at the surface of 40 mm heavy plate, which significantly increased the strength and decreased the elongation. Simultaneously, microstructural evolution in hot-rolled sheets was studied *via* simulation experiments using laboratory rolling mill to define the limits of microstructural evolution that can obtained in the UFC process and develop an understanding of the evolved microstructure in terms of process parameters.

DOI: 10.1007/s11661-015-2933-1

BIN WANG, Post-doctor, ZHAO-DONG WANG, Professor, BING-XING WANG, Lecturer, and GUO-DONG WANG, Academician, are with the State Key Laboratory of Rolling and Automation, Northeastern University, Shenyang 110819, P.R. China. Contact E-mail: wangbin404@126.com R.D.K. MISRA, Professor, is with the Center for Structural and Functional Materials Research and Innovation and Department of Metallurgical and Materials Engineering, University of Texas at El Paso, El Paso, TX 79968-0521.

Manuscript submitted January 19, 2015.
Article published online April 30, 2015

Thermomechanical controlled processing (TMCP) involving ultra fast cooling (UFC) technology is being currently applied to industrial production,[1–3] with the aim to reduce the consumption of alloying elements and make the steel making process economically viable.[4,5]

Heavy plate products of C-Mn steel are processed by TMCP for structural applications.[6] However, there is difficulty in obtaining uniform microstructure in heavy plates because of non-uniform deformation and non-uniform distribution of accelerated cooling along the thickness direction that leads to inhomogeneous microstructure across the plate thickness.[7,8]

In order to obtain near-uniform microstructure and similar mechanical properties from the surface to the center of plate, fast and effective cooling process is necessary. In this regard, the ongoing developments in UFC technology,[9,10] with strict control and faster cooling rate on the run-out table, provides a high degree of undercooling and potential for control of microstructure and phase transformation in water-cooled plates during the cooling process.[11]

In the present study, the potential of UFC in the processing of C-Mn heavy plates together with reduction in Mn-content is illustrated. UFC factors such as UFC stop temperature and the accompanying relationship between microstructural evolution, mechanical properties, and cooling rate is elucidated.

The nominal chemical composition of steel (in wt pct) was Fe-0.16 pctC-0.18 pctSi-1.0 pctMn-0.015 pctP-0.003 pctS. Heavy steel plates of 20 and 40 mm thickness were industrially processed using the UFC process. Keeping in mind the microstructural and mechanical property benefits that may be derived from the UFC process, Mn-content was reduced by ~0.3 to 0.5 wt pct in relation to the conventional composition of 1.3 to 1.5 pct specified in grade Q345B steel. The rolling temperature was ~1373 K (1100 °C) and finishing rolling temperature was controlled at ~1123 K (850 °C). The parameters of hot rolling for 20 mm plate are presented in Figure 1. The start-cooling and stop-cooling temperature of UFC was ~1073 K and 873 K (800 °C and 600 °C), respectively.

To define the limits or boundaries of microstructural evolution that can be obtained in UFC, simulation experiments were carried out using Φ450 mm experimental rolling mill equipped with ultra fast cooling equipment. Here sheets were processed rather than plates because of the load capacity of the mill. The microstructural evolution experienced in sheets during the UFC process can be considered as the ultimate limit in heavy plates. Different UFC stop temperatures were considered in the simulation experiment and the surface temperature of plate was measured by infrared thermal imaging equipment with the temperature range of 223 K to 1273 K (−50 °C to 1000 °C) and accuracy of 1.5 pct of reading or ±1.5 K and the repeatability of 1 pct of reading or ±1 K.

Metallography specimens for microstructural examination were prepared by grinding, polishing, and etching with 4 pct nital solution. The microstructure of the specimens was observed using a combination of optical microscope (OM—LEICA DMIRM), scanning electron microscope (SEM—ZEISS ULTRA 55), and electron microprobe (EPMA—JXA 8530F). Thin foils were prepared for the observation of fine cementite in transmission electron microscope (TEM TECNAI-G^2) by twin-jet electropolishing. The electrolyte was 10 pct (volume fraction) perchloric acid in methanol, maintained at 248 K (−25 °C) (potential of 30 V, and current of 45 mA.).

Standard tensile tests were carried out in the longitudinal direction using a SANS tensile testing machine at a cross-head speed of 3 mm/min. Charpy v-notch impact tests (heavy plate) were carried out using samples of dimensions 5 mm × 10 mm × 55 mm *via* a JBW-500 impact testing machine.

Tensile properties of industrially processed 20-mm-thick plate of C-Mn steels processed *via* UFC, namely, yield strength, tensile strength, pct elongation, and toughness at 293 K (20 °C), were 386 ± 10 MPa, 518 ± 15 MPa, 25 ± 2 pct, and 202 ± 20 J, respectively, which met the mechanical property standard of Q345B steel. In order to verify the uniformity of mechanical property in the whole plate, at least three samples were prepared for the full-thickness tensile test.

Microstructure across the thickness of 20 mm plate, as observed by OM and SEM, is presented in Figures 2 and 3, respectively. The microstructure was nearly homogeneous in the thickness direction and consisted of ferrite and pearlite (Figure 2), without banded structure forming in the microstructure, although the volume fraction of ferrite increased from the surface to the center of the plate. More importantly, from Figure 3(a), it can be seen that fine-scale precipitation of cementite occurred at the surface of plate (see below for TEM) as compared to the traditional lamellar pearlite structure. However, the cementite particles were relatively coarse at one-quarter thickness from the surface (Figure 3(b)) and lamellar in morphology at mid-thickness of plate (Figure 3(c)).

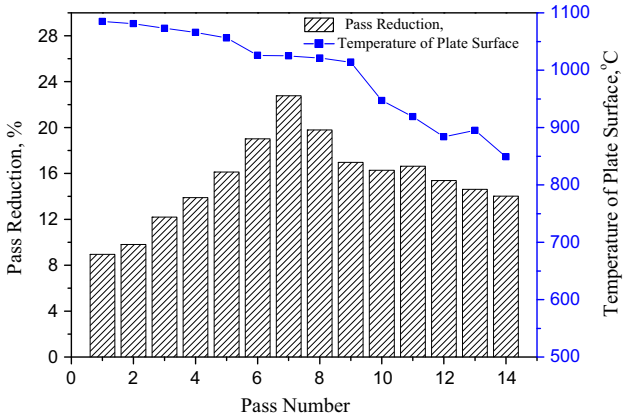

Fig. 1—Process parameters for hot rolling for 20 mm steel plate.

The TEM micrograph of cementite precipitates is presented in Figure 4, and the cementite particles are less than ~100 nm and distributed randomly in the microstructure. The chemical analysis of precipitates by energy dispersive X-ray spectroscopy in TEM confirmed

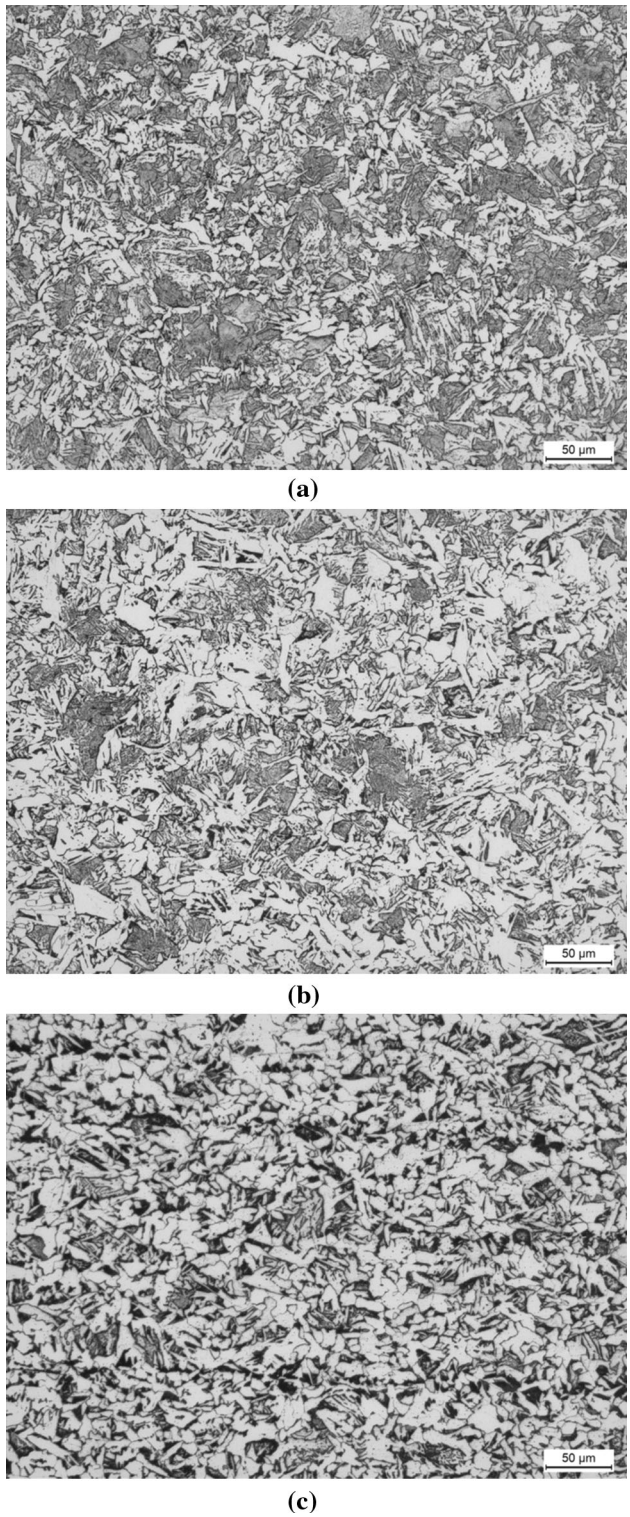

Fig. 2—Optical micrographs of 20 mm plate (*a*) surface (*b*) quarter thickness from the surface and (*c*) center.

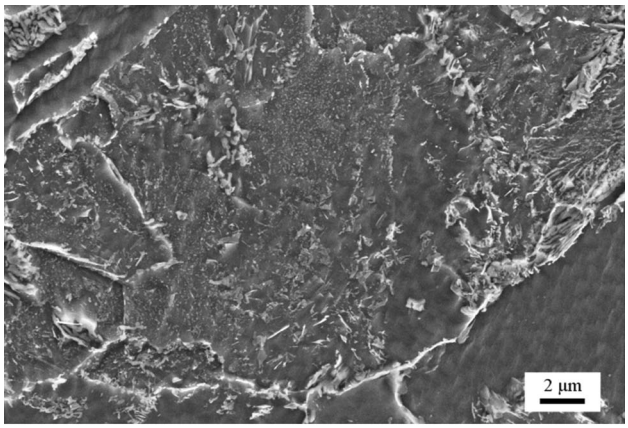

(a)

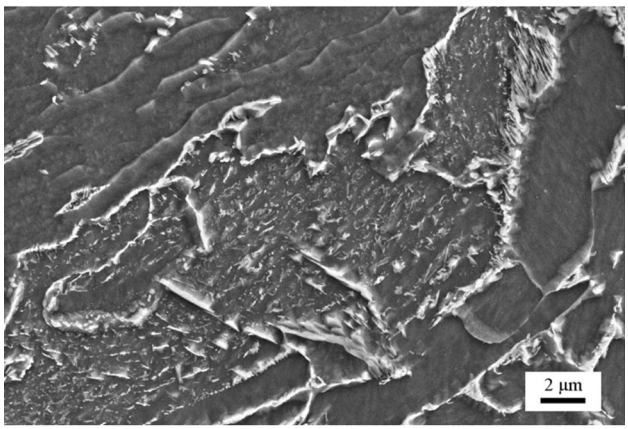

(b)

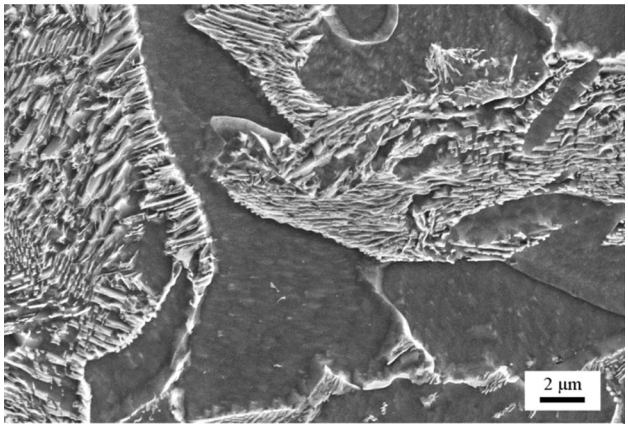

(c)

Fig. 3—SEM micrographs of 20 mm plate (*a*) surface (*b*) quarter thickness from the surface and (*c*) center.

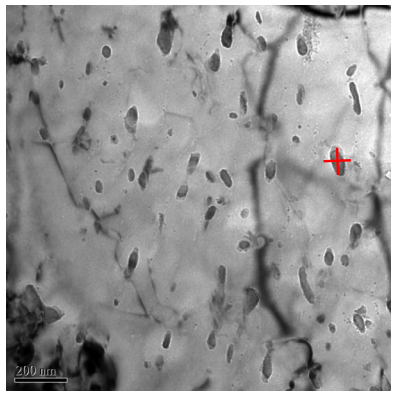

(a)

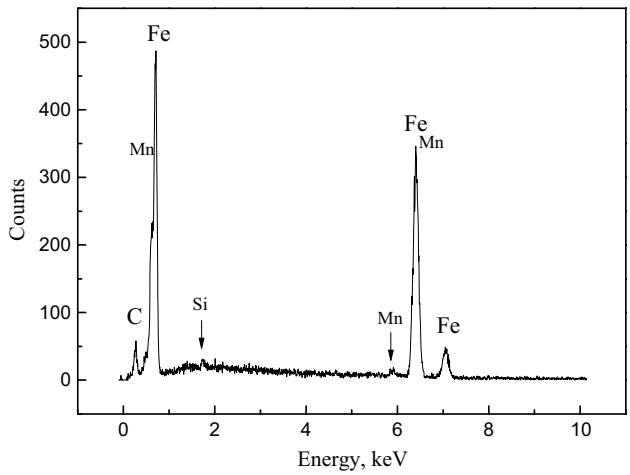

(b)

Fig. 4—(*a*) Bright-field TEM micrograph of nanoscale cementite precipitated at the surface and (*b*) energy dispersive analysis of cementite.

the presence of carbon-containing particles (Figure 4(b)). Figure 5 shows the elemental distribution for nanoscale cementite precipitates, as studied by EPMA. It reveals that the diffusion of interstitial element C was restrained by UFC such that the nanosize cementites were precipitated, instead of conventional lamellar morphology in pearlite phase. The non-carbide forming element Si, indicated an opposite distribution compared to C, and the substitutional element Mn was uniformly dispersed with no obvious segregation taking place during UFC process.

In simulation experiments with hot-rolled steel sheets, slabs were rolled from 70 to 7 mm thickness *via* nine passes by Φ450 mm rolling mill in the laboratory. The start rolling temperature was ~1373 K (1100 °C) and the finish rolling temperature was controlled to be ~1163 K (890 °C). Pass reduction was below 10 and 15 pct for the first and last two passes, respectively, while the pass reduction for the middle pass was greater than 15 pct. The variation in temperature and pass reduction for each pass during hot rolling was consistent with the process parameters of industrial trial (Figure 1). The hot-rolled strips were subjected to UFC process with the stop-cooling temperature in the range of 853 K to 1013 K (580 °C to 740 °C). Figure 6 is a schematic of the hot rolling experimental procedure.

The TEM micrographs of cementite in the experimental steels after hot rolling with different UFC stop temperatures are presented in Figure 7. The Figure 7 shows that cementite morphology changes from the lamellar structure to nanosized precipitates with decrease in the UFC stop temperature, which is consistent

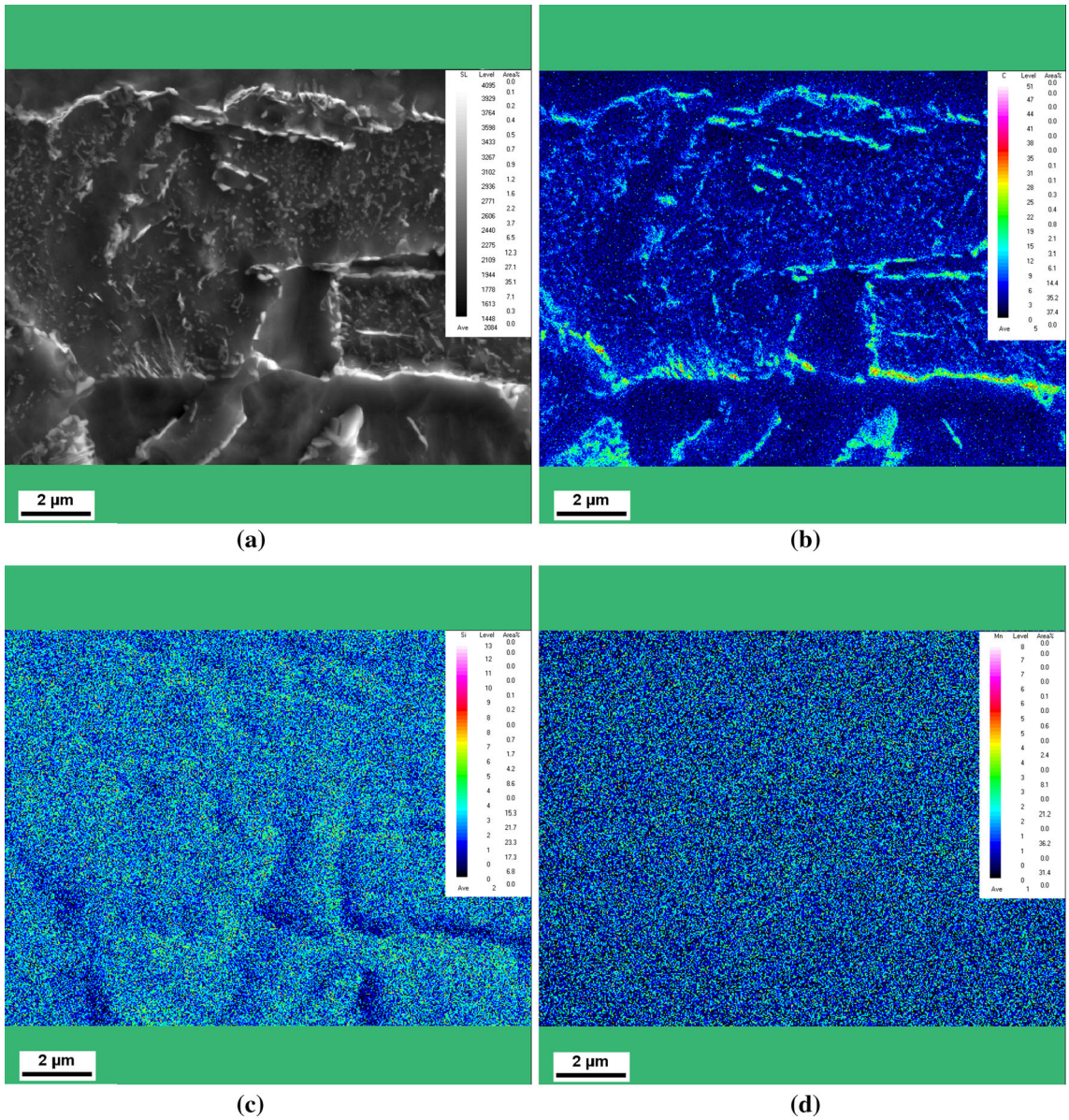

Fig. 5—(*a*) Microstructure of nanoscale cementite and elemental distribution of (*b*) Carbon (*c*) Silicon and (*d*) Manganese in nanoscale cementite precipitation area.

with the microstructural transition trend observed in the plate from the surface to the mid-thickness, processed through UFC.

Figure 8 summarizes tensile data for experimental sheets after hot rolling with different UFC stop temperatures. It can be seen that both yield strength and tensile strength increased with decrease in the UFC stop temperature, while the total elongation decreased with decrease in UFC stop temperature, confirming that the nanoscale cementite precipitation (Figure 7) is beneficial for strengthening.

In the industrially processed 40 mm C-Mn steel plate, the start and finish rolling temperature was controlled to be ~1373 K and 1123 K (1100 °C and 850 °C), respectively. The hot rolling parameters of 40 mm plate are presented in Figure 9. Hot-rolled heavy plate after rolling was subjected to UFC process with stop-cooling temperature of 753 K (480 °C), but the surface temperature of plate increased to 883 K (610 °C) in several seconds, because of the heat transfer from the mid-thickness of the plate to the surface.

Tensile properties including yield strength, tensile strength, pct elongation, and toughness at 293 K (20 °C) for 40 mm plate by UFC were 397 ± 15 MPa, 516 ± 20 MPa, 26 ± 2 pct, and 189 ± 25 J, respectively, which also met mechanical property standard for Q345B heavy plate.

Light and SEM micrographs across the thickness of 40 mm plate are presented in Figures 10 and 11, respectively. The bainite lath with nanosized dispersed cementite precipitates was formed at the surface, while the microstructure in other region consisted of ferrite

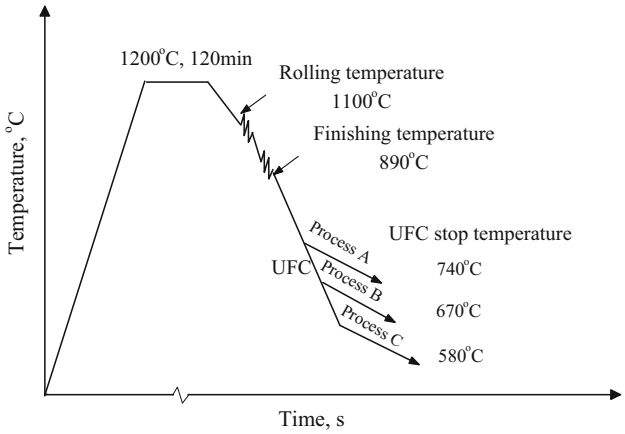

Fig. 6—Experimental procedure for ultra fast cooling (UFC) process of steel.

and pearlite (cementite with the similar structure described above. *i.e*. nanoscale precipitation).

UFC process and the following thermomechanical treatment experiment were carried out to simulate the formation of bainite lath layer with uniform cementite precipitation. Experiment slabs were hot-rolled from 70- to 7-mm-thick strips *via* nine passes on the laboratory mill. Next strips were subjected to UFC after finish rolling, and the UFC stop temperature was controlled to be 773 K (500 °C). Subsequently, plastic deformation from 7 to 6.5 mm was given in a single pass, holding for 20 minutes at 773 K (500 °C). Finally, strips were cooled to room temperature in air. Figure 12 shows a schematic of the hot rolling experiment to simulate the surface condition in the 40 mm plate.

High magnification SEM micrographs of bainite in the hot-rolled 40 mm plate and sheet for the simulated surface condition of the 40 mm plate are presented in Figure 13. The microstructure in simulated surface condition of 40 mm plate was lath-type bainite. In comparison to the surface microstructure of the hot-rolled plate, the presence of high degree of deformation and longer holding time in the simulation experiment of sheet led to the precipitation of a higher density of nanoscale cementite, which is the limit condition (significant deformation, faster cooling rate, and longer holding time) for hot-rolled plate.

Figure 14 summarizes the engineering stress–strain plots for experimental sheets for different hot rolling processes. The strength was significantly improved after UFC and thermomechanical processing. However, the elongation decreased with increasing strength, as expected.

The salient features of UFC technology briefly are (a) reduction in the diameter of cooling outlet and increase in the number of outlets for improving the uniformity in cooling, (b) increase of water pressure for cooling with tilt jet for flow to have adequate energy and impact to break the vapor film present between the water and steel surface. In view of the above characteristics, there is more fresh water directed on the steel surface per unit time to achieve a comprehensive nuclear boiling rather

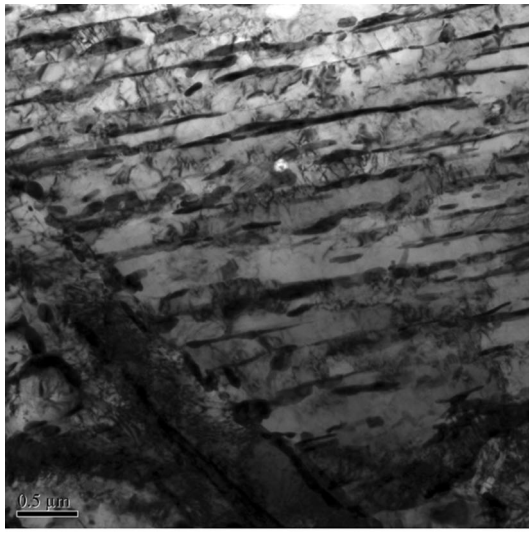

(a)

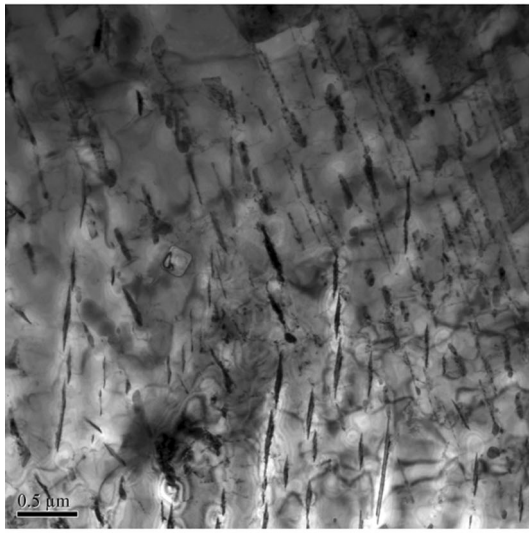

(b)

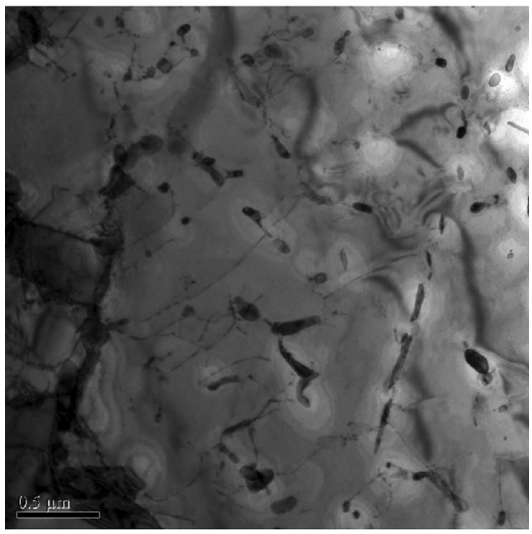

(c)

Fig. 7—Typical TEM morphology of cementite precipitation with different UFC stop temperatures (*a*) 1013 K (740 °C), (*b*) 943 K (670 °C), and (*c*) 853 K(580 °C).

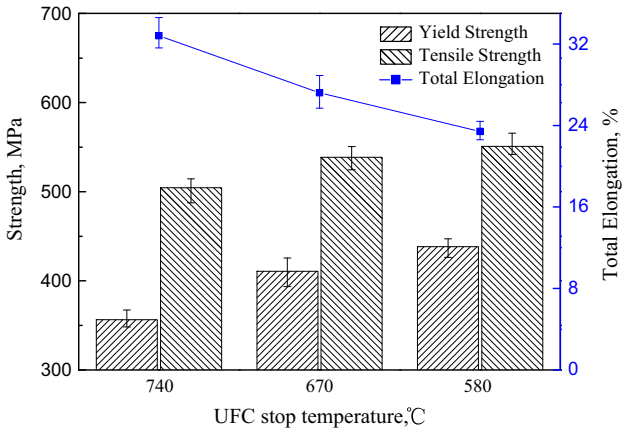

Fig. 8—Effect of UFC stop temperature on mechanical properties of hot-rolled sheet.

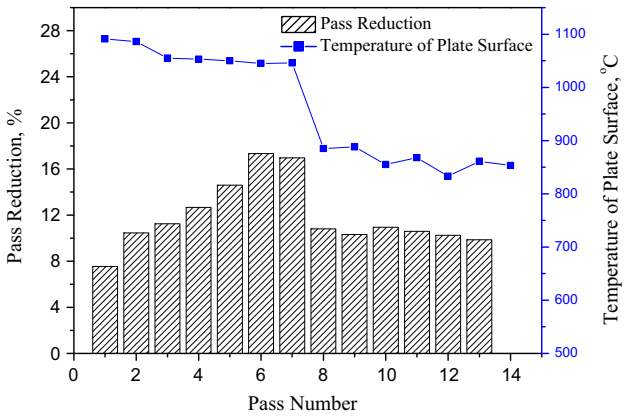

Fig. 9—Processing parameters of hot rolling for 40 mm steel plate.

than film boiling.[12–17] The above are the reasons why UFC technology can achieve very fast cooling effect on the surface by forced convection and heat transfer. However, the cooling process is achieved by heat conduction inside the plate, and cooling effect slows down with increase in thickness.[18,19] Thus, the temperature gradient along the thickness of plate needs consideration.

According to the cooling conditions during the UFC process, the steel plate was considered as an infinite flat plate without the internal heat source. Only considering the temperature change in the thickness direction and ignoring changes in the width and length direction, the calculation model was simplified as a one-dimensional unsteady heat conduction differential equation:

$$\frac{\partial T}{\partial \tau} = a\frac{\partial^2 T}{\partial x^2}(0 < x < d, \tau > 0), \qquad [1]$$

where T is absolute temperature, K; τ is time, s; x is the distance from the surface, mm; d is plate thickness, mm; $a = \frac{\lambda}{\rho c_p}$, namely thermal diffusivity; λ is the thermal conductivity, W/(m K); c_p is specific heat capacity, J/(kg K), ρ is density of steel, 7850 kg/m^3.

Heat transferring condition on the surface can be given by

$$-\lambda\frac{\partial T(x,\tau)}{\partial x}|_{x=0} = \alpha_x[T(0,\tau) - T_f] \ (\tau > 0), \qquad [2]$$

where T_f is the water temperature; α_x is heat transfer coefficient, W m^{-2} K^{-1}, which can be fitted from the experience date, such as flow intensity of water q (L m^{-2} min^{-1}) and surface temperature T,

$$\alpha_x = 1.078 \times 10^5 \times q^{0.43068}e^{-0.00935T}. \qquad [3]$$

Based on the UFC database model, the temperature plots of steel plate were calculated and simulated, and gradients in temperature and cooling rate through 20 mm plate are presented in Figure 15.

It can be seen that the cooling rate at the surface of the plate is significantly faster than in the mid-thickness during the UFC process, such that the UFC stop temperature is lower on the surface. In UFC, the austenite transformation temperature at the surface of the plate decreases significantly with increase in cooling rate, and a high degree of undercooling is obtained with consequent increase in free energy difference, which provides a higher driving force to accelerate the interface speed during austenite transformation.[20,21]

Meanwhile, the application of UFC reduces the transformation temperature and time to some extent such that rate of diffusion of carbon decreases significantly and the supply of carbon atoms is insufficient. The diffusion of carbon is limited in undercooled austenite and the cementite growth is controlled by diffusion of carbon. If the carbon diffusion rate is less than the moving speed of the interface, then the cementite cannot grow continuously to form a lamellar structure, but precipitates as nanosized particles, in the special case of eutectoid decomposition. But if the diffusion rate of carbon is greater than the moving speed of interface and the carbon atoms are adequately available, cementite forms as a continuous lamellar morphology.[22]

It was proven in hot rolling experiments of sheets that cementite morphology is consistent with the UFC stop temperature, and the lower stop-cooling temperature with fast cooling rate promoted the formation of nanoscale cementite. Additionally, nanoscale cementite contributes to the precipitation strengthening of C-Mn steel, and the effect increases with the decrease in the UFC stop temperature.

When the plate thickness increases, although the cooling condition between the surface and the fluid does not significantly change, the cooling in the mid-thickness of the plate is weak. Thus, the surface effect of heavy plate merits consideration.

In Figure 16 are presented the temperature curves of 40 mm plate during the cooling process. There is significant variation in surface temperature during the cooling process. The cooling rate on the surface is very fast and the temperature decreases during the UFC process, and increases rapidly after water-cooling because of the heat transferred from the mid-thickness to the surface.

(a)

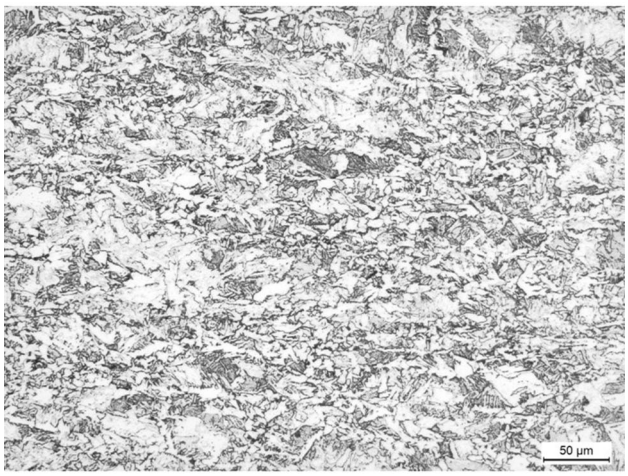

(b)

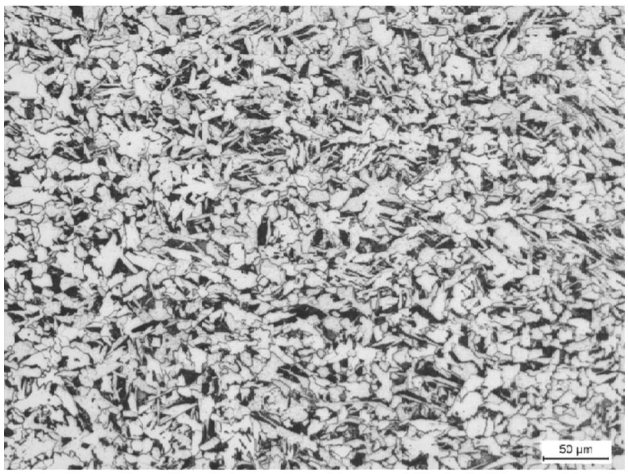

(c)

Fig. 10—Optical micrographs of 40 mm plate. (*a*) surface (*b*) quarter thickness from the surface and (*c*) center.

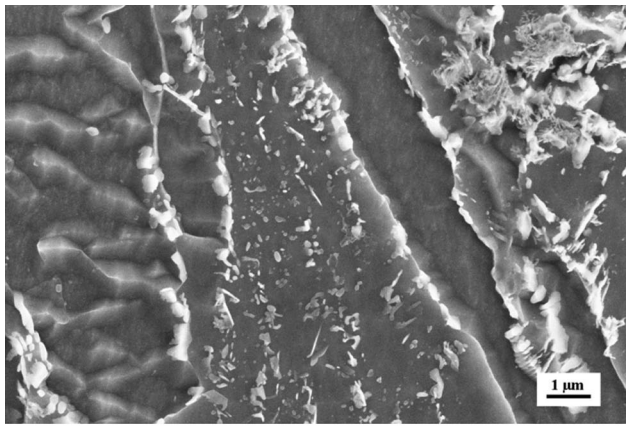

(a)

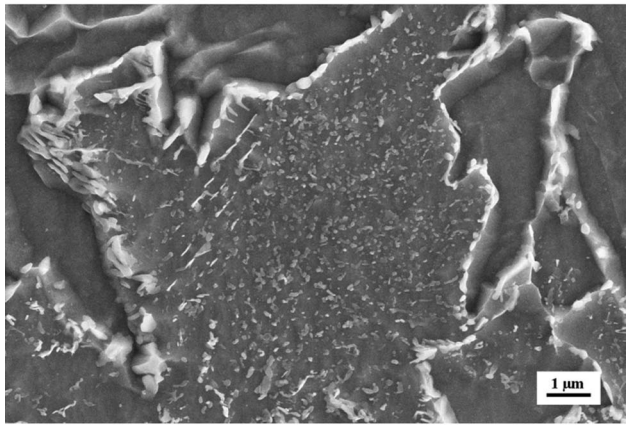

(b)

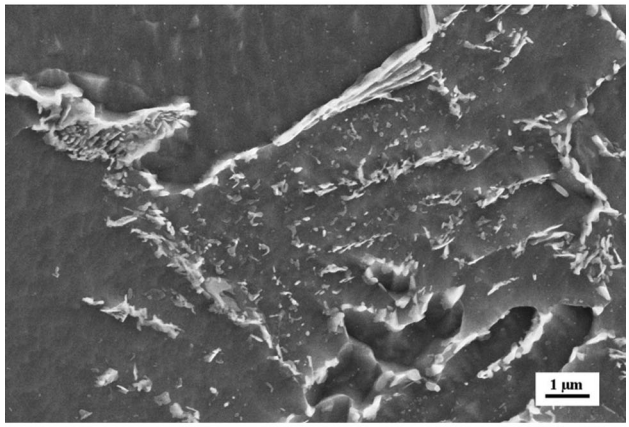

(c)

Fig. 11—SEM micrographs of 40 mm plate (*a*) surface (*b*) quarter thickness from the surface and (*c*) center.

When the surface is cooled directly from austenite through the two-phase region and eutectoid decomposition temperature to bainite region, bainite begins to form depending on the cooling rate. During transformation of austenite to bainite, the element, C, is supersaturated in bainite, because there is no time for carbon diffusion in the UFC process and the diffusion coefficient of carbon decreases as the temperature falls.

After the cooling process, the surface gets reheated in the pearlite region for some time by the heat transferred from the mid-thickness, and the supersaturation of carbon in bainite begins to precipitate in the form of cementite particles. At this time, the deformation can increase the nucleation rate of cementite by strain-

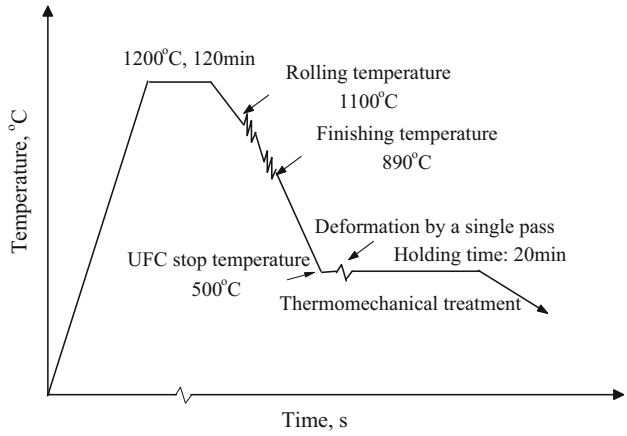

Fig. 12—Experimental procedure for ultra fast cooling (UFC) and thermomechanical treatment of steel.

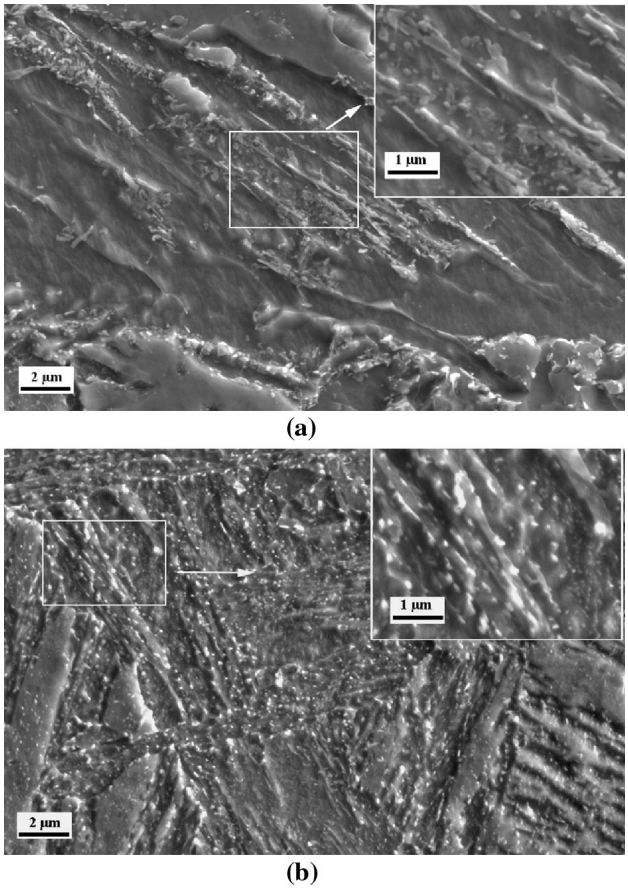

Fig. 13—SEM micrograph of bainite layer with nanoscale cementite precipitation in (*a*) plate and (*b*) hot-rolled sheet.

induced precipitation and the holding process will provide adequate time for cementite to precipitate.[23–25] This result was also confirmed by thermomechanical processing of experiment of steel sheets such that a large number of nanoscale cementites precipitated in lath bainite after plastic deformation and holding process.

In fact, during hot rolling, the austenite becomes work hardened because of high degree of deformation

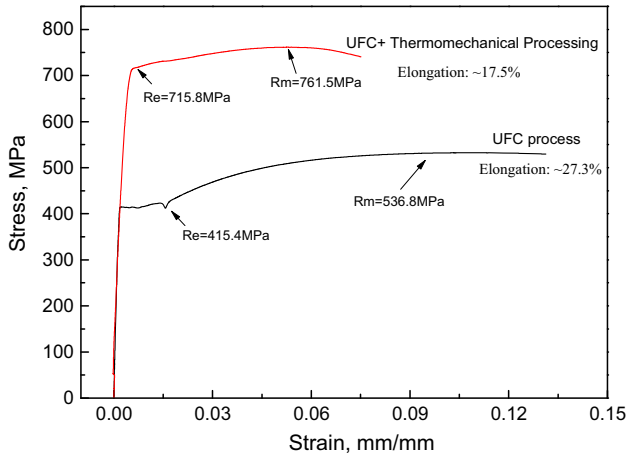

Fig. 14—Tensile stress–strain plots for different hot-rolled processes.

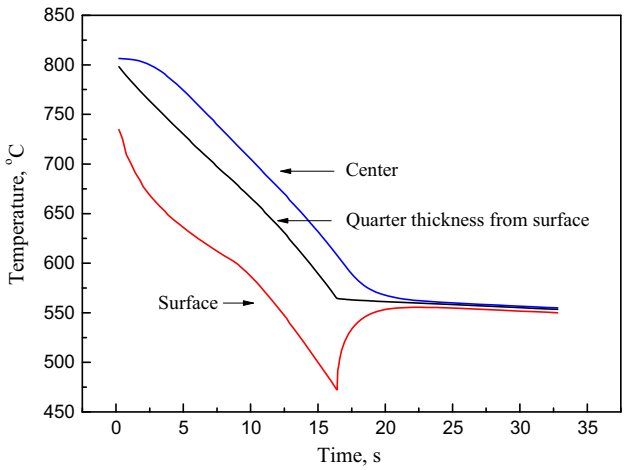

Fig. 15—Temperature plots of 20 mm plate during the cooling process.

and strain accumulation at the surface compared to the center.[26–28] In the UFC process, at the surface, a number of dislocations are retained and deformation energy is stored, as shown in Figure 17. During the surface reheating process after UFC (*i.e.*, when the heat is transferred from the mid-thickness to the surface and the surface temperature increases, as shown in Figure 16, which corresponds to the holding time in Figure 12), dislocations are paths for diffusion of carbon and provide favorable sites for nucleation of cementite, and the stored deformation energy also provides the necessary driving force for cementite precipitation.[29,30]

The research described here provides an exciting new prospect in the processing of carbon steels with nanoscale cementite. The UFC technology developed by RAL, with the high cooling capacity and high precision control was successfully applied after the hot rolling experiments to obtain cementite precipitation and understand the mechanism of formation. When cementite is effectively refined to the scale of a few nanometers, it provides significant precipitation

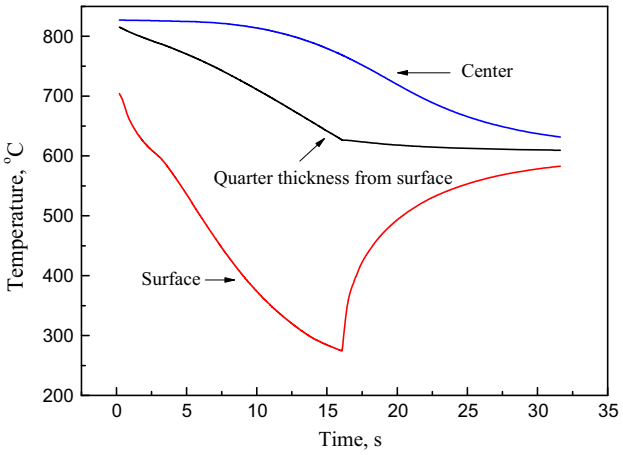

Fig. 16—Temperature curves of 40 mm plate during the cooling process.

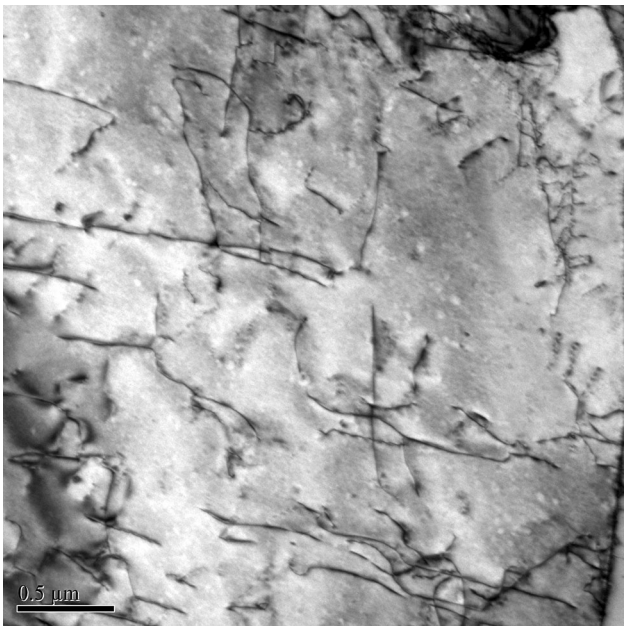

Fig. 17—TEM micrograph of dislocations during UFC process.

strengthening effect. Thus, cementite is viewed as a viable option to replace precipitates of microalloying elements and consequently reduce the alloy cost and maintain strength.

Our future and current research effort is aimed at optimizing the processing parameters for nanoscale cementite precipitation in low and middle carbon steels. Furthermore, the microstructural evolution and mechanism of nanoscale cementite in a non-equilibrium state will be elucidated, together with the establishment of precipitation model. The impact of research is far reaching because of the need to pioneer a new frontier of high strength-low cost carbon steels for engineering applications.

Application of UFC technology is also important from other perspectives. For instance, 0.1 wt pct reduction in manganese in steel will save ~$1.5/ton in industrial production cost. In this research, the reduction in Mn-content was ~0.3 to 0.5 pct, which is expected to increase the profit margin by ~$6/ton. The crude steel production of China reached 822.7 million tons in 2014. Industrial application of the research described here would provide significant economic benefit.

It is also pertinent to indicate that the effective control of cooling path during the UFC process is currently being applied to a wide range of microalloyed steels for varied applications that include line pipe and off-shore platforms steels, to list a few.

1. A high density of nanoscale cementites precipitates during austenite transformation in the heavy plate during the ultrafast cooling process, which provides precipitation strengthening.
2. The lower UFC stop-cooling temperature at fast cooling rate promotes the formation of nanoscale cementite. From the surface to mid-thickness, there was a transition in the morphology of cementite from nanoscale particles to lamellar structure in the 20 mm heavy plate during the UFC process.
3. The thin layer of lath bainite with nanoscale cementite at the surface of the 40 mm plate enhances strength and decreases elongation.
4. The fast cooling rate, the low UFC stop-cooling temperature, large deformation, and reheating process plays a determining role in the formation of lath bainite with nanoscale cementite precipitates in the surface of the heavy plate.

The research was supported financially by National Natural Science Foundation of China, Fundamental Research Funds for the Central Universities, and Chinese Postdoctoral Science Foundation through grant numbers 51234002, N130307001, and 2014M551107, respectively. One of the authors (RDKM) greatly acknowledges support from the University of Texas at El Paso.

REFERENCES

1. A. Lucas, P. Simon, and G. Bourdon: *Steel Res. Int.*, 2004, vol. 75, pp. 139–46.
2. P. Simon, J.P. Fishbach, and P. Riche: *Revue De Metall.*, 1996, vol. 93, pp. 409–15.

3. H.J. Li, Z.L. Li, G. Yuan, Z.D. Wang, and G.D. Wang: *J. Iron. Steel Res. Int*., 2013, vol. 20, pp. 29–34.
4. G.D. Wang: *Shanghai Met*., 2008, vol. 30, pp. 1–4.
5. G.D. Wang, X.H. Liu, L.G. Sun, Z. Liu, and D.Q. Liu: *Iron Steel*, 2008, vol. 43, pp. 49–52.
6. K. Nishioka and K. Ichikawa: *Sci. Technol. Adv. Mater*., 2012, vol. 13, pp. 1–20.
7. K.F.A. Hajeri, C.I. Garcia, M. Hua, and A.J. DeArdo: *ISIJ Int*., 2006, vol. 46, pp. 1233–40.
8. C. Capdevila, C. Garcia-Mateo, J. Chao, and F.G. Caballero: *Mater. Sci. Technol*., 2009, vol. 25, pp. 1383–86.
9. G. Buzzichelli and E. Anelli: *ISIJ Int*., 2002, vol. 42, pp. 1354–63.
10. X.H. Liu, L.G. Peng, and G.D. Wang: *Iron Steel*, 2004, vol. 39, pp. 71–74.
11. Y.V. Leeuwe, M. Onink, J. Sietsm, and S. van der Zwagg: *ISIJ Int*., 2001, vol. 41, pp. 1037–46.
12. E.Y. Liu, L.G. Peng, G. Yuan, Z.D. Wang, D.H. Zhang, and G.D. Wang: *J. Cent. South Univ. T*., 2012, vol. 19, pp. 1341–45.
13. B. Wang, Y. Tian, G. Yuan, Z. Wang, G. Wang, and J. Chen: *Manuf. Process Tech*., 2011, vols. 189–193 (Pts 1–5), pp. 2515–21.
14. H. Kagechika: *ISIJ Int*., 2006, vol. 46, pp. 939–58.
15. B.X. Wang, Q. Xie Qian, Z.D. Wang, and G.D. Wang: *J. Cent. South Univ*., 2013, vol. 20, pp. 2960–66.
16. B.X. Wang, X.L. Chen, Y. Tian, Z.D. Wang, J. Wang, and D.H. Zhang: *J. Iron. Steel Res. Int*., 2011, vol. 28, pp. 38–41.
17. P. Bhattacharya, A.N. Samanta, and S. Chakraborty: *Int. J. Therm. Sci*., 2009, vol. 48, pp. 1741–47.
18. G.N. Praveen and J.N. Reddy: *Int. J. Solids Struct*., 1998, vol. 35, pp. 4457–76.
19. X.I. Chen, G.D. Wang, Y. Tian, B.X. Wang, G. Yuan, and Z.D. Wang: *J. Iron. Steel Res. Int*., 2014, vol. 21, pp. 481–87.
20. B. Wang, Z.Y. Liu, X.G. Zhou, and G.D. Wang: *Acta Metall. Sin*., 2013, vol. 49, pp. 26–34.
21. H. Yin, T. Emi, and H. Shibata: *ISIJ Int*., 1998, vol. 38, pp. 794–801.
22. B. Wang, Z.Y. Liu, X.G. Zhou, G.D. Wang, and R.D.K. Misra: *Mater. Sci. Eng. A*, 2013, vol. 575, pp. 189–98.
23. R.L. Klueh, N. Hashimoto, and P.J. Maziasz: *Scripta Mater*., 2005, vol. 53, pp. 275–80.
24. S.N. Prasad and D.S. Sarma: *Mater. Sci. Eng. A*, 2005, vol. 399, pp. 161–72.
25. D. Rojas, J. Garcia, O. Prat, L. Agudo, C. Carrasco, G. Sauthoff, and A.R. Kaysser-Pyzalla: *Mater. Trans. A*, 2011, vol. 528A, pp. 1372–81.
26. S. Choi, Y. Lee, P.D. Hodgson, and J.S. Woo: *J. Mater. Process. Technol*., 2002, vol. 125, pp. 63–71.
27. R.S. Nalawade, A.J. Puranik, G. Balachandran, K.N. Mahadik, and V. Balasubramanian: *Int. J. Mech. Sci*., 2013, vol. 77, pp. 8–16.
28. J.L. Zhang and Z.S. Cui: *J. Iron. Steel Res. Int*., 2011, vol. 18, pp. 20–27.
29. S.N. Prasad and D.S. Sarma: *Mater. Sci. Eng. A*, 2005, vol. 408, pp. 53–63.
30. H. Jafari, M.H. Idris, A. Ourdjini, and G. Payganeh: *Acta Metall. Sin. (English Letters)*, 2009, vol. 22, pp. 401–407.